DISCRETE AND CONTINUOUS
DYNAMICAL SYSTEMS SERIES B
Volume **23**, Number **7**, September **2018**

doi:10.3934/dcdsb.2018103

pp. **2743–2762**

PERIODIC ORBITS OF PLANAR DISCONTINUOUS SYSTEM UNDER DISCRETIZATION

Luca Dieci

School of Mathematics, Georgia Tech
Atlanta, GA 30332, USA

Timo Eirola

Dept. of Mathematics and Systems Analysis, Aalto University
Espoo, FI-00076, Finland

Cinzia Elia

Dipartimento di Matematica, Univ. of Bari
I-70100, Bari, Italy

Abstract. We consider a model planar system with discontinuous right-hand side possessing an attracting periodic orbit, and we investigate what happens to a Euler discretization with stepsize τ of this system. We show that, in general, the resulting discrete dynamical system does not possess an invariant curve, in sharp contrast to what happens for smooth problems. In our context, we show that the numerical trajectories are forced to remain inside a band, whose width is proportional to the discretization stepsize τ. We further show that if we consider an event-driven discretization of the model problem, whereby the solution is forced to step exactly on the discontinuity line, then there is a discrete periodic solution near the one of the original problem (for sufficiently small τ). Finally, we consider what happens to the Euler discretization of the regularized system rewritten in polar coordinates, and give numerical evidence that the discrete solution now undergoes a period doubling cascade with respect to the regularization parameter ϵ, for fixed τ.

1. Periodic orbit of a planar system with discontinuous right-hand side under discretization. Regularized problem and period doubling cascade.

We consider the following model of discontinuous system of differential equations

$$\frac{d}{dt}\begin{bmatrix}x\\y\end{bmatrix} = \begin{cases} \begin{bmatrix} c & d\\ -d & c\end{bmatrix}\begin{bmatrix}x\\y\end{bmatrix}, & y < m\,,\\ \begin{bmatrix} -a & b\\ -b & -a\end{bmatrix}\begin{bmatrix}x\\y\end{bmatrix}, & y > m\,, \end{cases} \tag{1}$$

where $a, b, c, d, m > 0$. Without loss of generality, we can take $m = 1$, as we will often do in this work. Motion always takes place forward in time, and thus proceeds clockwise.

This sytem was studied in [4], where it was shown that, for $\frac{a}{b} > \frac{c}{d}$, (1) has a globally (aside for the origin) asymptotically stable limit cycle of crossing type:

2010 *Mathematics Subject Classification.* 65L99, 34A36, 37N30.

Key words and phrases. Discontinuous planar system, periodic orbit, Euler method.

Discussion on this work begun while the last two authors were visiting the School of Mathematics of Georgia Tech in Spring 2015, and it is dedicated to the memory of our beloved friend and co-author Timo Eirola who unfortunately never saw the end of this work.

it consists of two smooth arcs above and below the line $y = m$, connecting into a periodic orbit transversed clockwise. Different bifurcation phenomena occurs as $\frac{c}{d}$ decreases towards 0 and the limit cycle changes from crossing, to crossing and sliding, to a sliding limit cycle.

In this work, we are interested in studying what happens to a Euler discretization of (1), insofar as the above mentioned crossing limit cycle.

A common means of studying (1) is to replace it with a smooth system, a *regularization* (e.g., see [8]). For this reason, in this work we will also consider the Euler discretization of the following smooth regularization of (1):

$$\frac{d}{dt}\begin{bmatrix} x \\ y \end{bmatrix} = (1 - g_\epsilon(z)) \begin{bmatrix} c & d \\ -d & c \end{bmatrix} \begin{bmatrix} x \\ y \end{bmatrix} + g_\epsilon(z) \begin{bmatrix} -a & b \\ -b & -a \end{bmatrix} \begin{bmatrix} x \\ y \end{bmatrix} , \tag{2}$$

where g_ϵ is an at least C^1 transition function. In this paper, we work with

$$g_\epsilon(z) = \begin{cases} 1 & z \geq \epsilon \\ \frac{1}{2} + \frac{z}{4\epsilon}\left(3 - (\frac{z}{\epsilon})^2\right) & -\epsilon < z < \epsilon \\ 0 & z \leq -\epsilon \end{cases} \quad \text{and } z = y - m \, . \tag{3}$$

(For the record, we have also used different choices of g_ϵ, for example a fifth degree polynomial, and obtained essentially the same result as we report in this work).

For small ϵ, one may expect that solutions of (2) resemble those of (1). This is effectively correct, and the following proposition holds.

Proposition 1. *For $\epsilon \geq \epsilon_0 > 0$ sufficiently small, and $\frac{a}{b} > \frac{c}{d}$, system (2) admits an asymptotically stable limit cycle. The limit cycle of (2) converges, as $\epsilon \to 0$, to that of (1).*

Proof. This is proven in [3] or [7]. □

Now, there are very refined general results on discretization of smooth dynamical systems (e.g., see [6] or [2]). In particular, the following result holds.

Theorem 2. [2, 6] *Let the smooth system $\dot{z} = f(z)$, $f \in \mathcal{C}^q$, $q \geq 1$, have a hyperbolic periodic orbit γ. Consider the discrete dynamical system obtained by a Runge Kutta discretization of order p, $p \leq q$, of the original problem: $z_{k+1} = z_k + \tau\Phi(\tau, z_k, f)$, $k = 1, 2, \ldots$. Then, for sufficiently small τ, the discrete dynamical system has an invariant closed curve Γ. Further, Γ has the same hyperbolicity type of the original periodic orbit, and it is $O(\tau^p)$-close to the original periodic orbit.* □

In this work we address the following questions.

(Q1) What survives of a result like Theorem 2 for the discontinuous dynamical system (1)?

(Q2) In which form does a result like Theorem 2 survive for the smooth system (2) as $\epsilon \to 0$?

We will provide answers to these questions relative to Euler method, the prototypical 1-step method. For example, for (1), the method reads

$$\begin{bmatrix} x_{k+1} \\ y_{k+1} \end{bmatrix} = \begin{cases} \left(I + \tau \begin{bmatrix} c & d \\ -d & c \end{bmatrix}\right) \begin{bmatrix} x_k \\ y_k \end{bmatrix} , & y_k < m \, , \\ \left(I + \tau \begin{bmatrix} -a & b \\ -b & -a \end{bmatrix}\right) \begin{bmatrix} x_k \\ y_k \end{bmatrix} , & y_k > m \, , \end{cases} \quad k = 0, 1, \ldots \, , \tag{4}$$

or more compactly as

$$\begin{bmatrix} x_{k+1} \\ y_{k+1} \end{bmatrix} =: \Phi(\tau) \begin{bmatrix} x_k \\ y_k \end{bmatrix} = \begin{cases} S_1(\tau) \begin{bmatrix} x_k \\ y_k \end{bmatrix} , & y_k < m , \\ \\ S_2(\tau) \begin{bmatrix} x_k \\ y_k \end{bmatrix} , & y_k > m , \end{cases} \tag{5}$$

with the provision that if $y = m$, then we will use S_1 if $x > \frac{c}{d}m$, and S_2 if $x < -\frac{a}{b}m$. We do not consider the case $-\frac{a}{b}m \le x \le \frac{c}{d}m$, since this is a sliding segment and we are only interested in solutions of (1) in a neighborhood of the crossing periodic orbit.

Furthermore, we will also consider the broken line interpolant resulting from Euler method; recall that this is nothing but the piecewise linear extension of Euler method:

$$\begin{bmatrix} x_k \\ y_k \end{bmatrix} + s \begin{bmatrix} x_{k+1} - x_k \\ y_{k+1} - y_k \end{bmatrix} , \quad 0 \le s \le 1 , \quad k = 0, 1, \dots .$$

We have to stress that, in spite of the deceiving simplicity of the model (1) and of the discretization method, the previously posed questions (Q1) and (Q2) are not at all trivial and the answers will be somewhat surprising.

In the remainder of this Section, first we look at what can be said when the system is rewritten in polar coordinates. Then, we will show results of several numerical experiments in support of our answers to questions (Q1) and (Q2). In Sections 2 and 3 we give our main theoretical results. Section 4 contains conclusions.

1.1. **Polar coordinates.** In our quest to answer questions (Q1) and (Q2) above, it will be useful to consider the polar coordinates rewriting of system (1). Trivially, in polar coordinates (1) rewrites as

$$\begin{pmatrix} \dot\rho \\ \dot\theta \end{pmatrix} = \begin{cases} \begin{pmatrix} c\rho \\ -d \end{pmatrix} , & \rho \sin\theta < m , \\ \\ \begin{pmatrix} -a\rho \\ -b \end{pmatrix} , & \rho \sin\theta > m . \end{cases} \tag{6}$$

From this, it is immediate to obtain:

$$\frac{d\rho}{d\theta} = \begin{cases} -\frac{c}{d}\rho , & \rho \sin\theta < m , \\ \frac{a}{b}\rho , & \rho \sin\theta > m . \end{cases} \tag{7}$$

Clearly, a periodic solution of (1) corresponds to a 2π-periodic solution (function) of (7).

Let $N > 0$ and choose a stepsize $\tau = \frac{2\pi}{N}$. Let $\theta_n = \theta_0 + n\tau$, for any fixed θ_0, and consider Euler's method with stepsize τ for (7). This gives the discontinuous map

$$\rho_{n+1} = \begin{cases} (1 - \tau\frac{c}{d})\rho_n , & \rho_n \sin\theta_n < m , \\ (1 + \tau\frac{a}{b})\rho_n , & \rho_n \sin\theta_n > m , \end{cases} \tag{8}$$

with the agreement that, if $\rho_n \sin(\theta_n) = m$, we will take $\rho_{n+1} = \begin{cases} (1 - \tau\frac{c}{d})\rho_n , & \rho_n \cos\theta_n > \frac{c}{d}m \\ (1 + \tau\frac{a}{b})\rho_n , & \rho_n \cos\theta_n < -\frac{a}{b}m \end{cases}$. Now, notice that for each $p > 0$, the values ρ_{N+p} must all belong to the same line $\theta = \theta_p$. As a consequence of this, if there is an invariant closed curve for the map (8) then it must be a periodic point for the map. This means that there must exist $k_1, k_2, \in \mathbb{N}$ so that

$$\left(1 - \tau\frac{c}{d}\right)^{k_1} \left(1 + \tau\frac{a}{b}\right)^{k_2} \rho_0 = \rho_0,$$

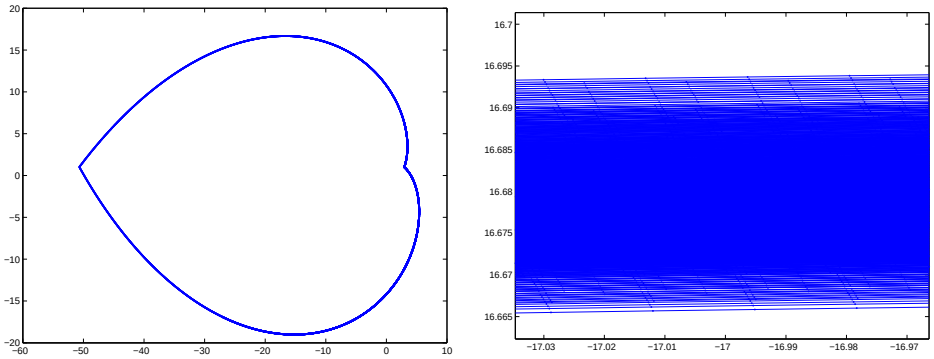

FIGURE 1. Euler trajectory on (1) and blow-up.

which we rewrite it as $-\frac{k_1}{k_2}\log(1-\tau\frac{c}{d}) = \log(1+\tau\frac{a}{b})$. For τ small, by taking the Taylor expansions of the two logarithms we obtain

$$-\frac{k_1}{k_2}\sum_{n=1}^{\infty}\frac{(-1)^{n+1}}{n}\left(-\tau\frac{c}{d}\right)^n = \sum_{n=1}^{\infty}\frac{(-1)^{n+1}}{n}\left(\tau\frac{a}{b}\right)^n \quad . \tag{9}$$

For these power series to be equal we need

$$\frac{k_1}{k_2} = \frac{a}{b}\frac{d}{c}, \quad \frac{k_1}{k_2} = -\frac{a^2}{b^2}\frac{d^2}{c^2}, \ldots$$

and this already gives a contradiction. Thus, the following theorem holds.

Proposition 3. *The discontinuous map* (8)*, with* $\tau = \frac{2\pi}{N}$*, and* $N \in \mathbb{N}$*, does not have a periodic point.* □

Remark 4. As a consequence of Proposition 3, there cannot exist a $\bar\tau$ sufficiently small such that for all $\tau \in (0, \bar\tau)$, Euler method applied to (7) has an invariant closed curve. This already tells us that well known results for smooth systems do not apply to discontinuous systems. But, it still does not tell us what survives of those results.

1.2. **Some experiments.** Below, we report on some numerical experiments aiming at understading the behavior of Euler method applied to (1).

Example 5. We consider (1), with parameter values $m = 1$, $a = b = d = 1$ and $c = 0.8$, for which (1) admits an asymptotically stable crossing limit cycle (see [4]). Next, we take a Euler discretization of (1) and see if (as it would be the case for a smooth problem for sufficiently small stepsize, see Theorem 2) there is an attracting invariant curve for the discrete map, near the limit cycle.

After discarding a transient, we observe that the numerical trajectory remains near the limit cycle, but there does not seem to be a closed curve for the numerical method. What we see is a "band-like region." See Figure 1 for Euler method with stepsize 5×10^{-4} and 20000 steps and a blow up when we take 10^7 steps. The band we see contains the periodic orbit of the system.

We made several more experiments with different random initial conditions and stepsizes, validating the following observations.

(i) The "band" fills-in, although we are not able to discern a mechanism of how it gets organized, which appears to be "chaotic."

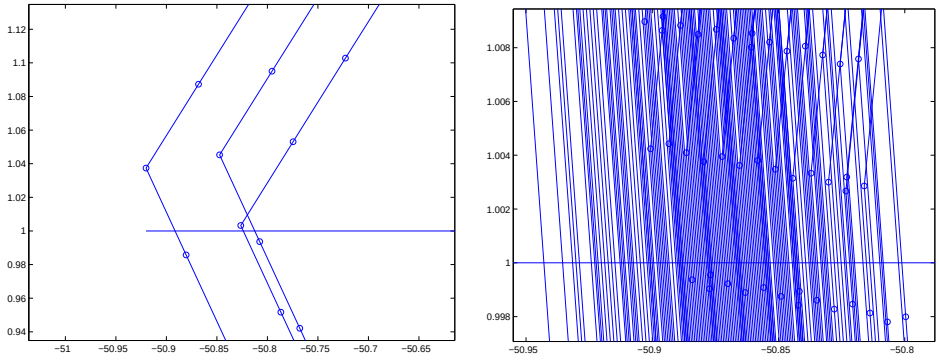

FIGURE 2. Exchange mechanism of Euler trajectories on (1); few iterates on the left figure, and many iterates on the right figure.

(ii) At the same time, decreasing τ shows that the bandwidth decreases linearly with τ.

Based on the above, we formulate the following claim, which we will prove in Section 3.

Claim 1. *For any given $\tau > 0$, bounded away from 0 and sufficiently small, and any cross section of the periodic orbit of (1), the piecewise linear interpolant of the Euler iterates –evaluated at the cross section– eventually remains in an interval of finite width $\omega(\tau)$. The width $\omega(\tau)$ depends on τ and on the cross section but not on the number of Euler iterates, and it decreases linearly in τ.*

Our experiments highlighted also the following behavior, which will be rigorously shown in Section 2, Lemma 12.

Claim 2. *Euler method on the upper and lower pieces is "monotóne," in the following sense.*

(a) Upper part. Suppose that at $y = 1$ we have two different values of x, say x_0 and $\widehat{x}_0$, with $x_0 < \widehat{x}_0$, both negative, and we integrate with Euler method the system (1), for as long as both y_k and $\widehat{y}_k$ remain greater than 1. Call $\gamma_{t,\tau}$ and $\widehat{\gamma}_{t,\tau}$ the two broken line interpolants associated to the respective Euler trajectories. Then, the Euler steps are monotone in the sense that the two interpolants do not cross each other, and $\gamma_{t,\tau}$ is above $\widehat{\gamma}_{t,\tau}$ (i.e., it is farther away from the origin).

(b) Bottom part. Again, suppose that at $y = 1$ we have two different values of x, say x_0 and $\widehat{x}_0$, with $x_0 < \widehat{x}_0$, both positive, and we integrate with Euler method the system (1), for as long as y_k and $\widehat{y}_k$ remain less than 1. Call $\gamma_{t,\tau}$ and $\widehat{\gamma}_{t,\tau}$ the two broken line interpolants associated to the respective Euler trajectories. Then, the Euler steps are monotone in the sense that $\gamma_{t,\tau}$ and $\widehat{\gamma}_{t,\tau}$ do not cross each other, and $\gamma_{t,\tau}$ is below $\widehat{\gamma}_{t,\tau}$ (i.e., it is farther away from the origin).

Now, assuming true Claim 2, the only mechanism by which Euler interpolants can cross each other is due to the way that they cross the line $y = 1$, on the right and the left. See Figure 2 for an illustration of this fact, relative to the left crossing of $y = 1$. A similar mechanism occurs relative to the right crossing of $y = 1$.

1.3. **Discretization of regularized problem in polar coordinates.** Next, consider the one-parameter map obtained applying Euler's method to (2) with stepsize τ. Then, Proposition 1 and Theorem 2 tell us that, for $\epsilon \geq \epsilon_0 > 0$, and sufficiently small, there exists a $\bar{\tau}_\epsilon > 0$ such that, for $\tau \in (0, \bar{\tau}_\epsilon)$, the discrete system admits an invariant closed curve γ_ϵ^τ, which is $O(\tau)$ close to the periodic orbit of (2), and converges to it as $\tau \to 0$. But, the caveat in this inference is in the term $O(\tau)$ which hides a constant that becomes unbounded as $\epsilon \to 0$. So, what happens as ϵ becomes smaller and smaller for a given τ?

Below, we give numerical evidence that, for τ fixed, the numerical method undergoes a period doubling cascade as ϵ decreases.

Remark 6. In the literature on discretized smooth systems, there are several results about possibly different behaviors between the original smooth dynamics, and the discretized one; e.g., see the discussion and references on spurious fixed points in [9]. However, the phenomenon on which we report here is very different from any other result of which we are aware; not only because of the nature of the phenomenon occurring (period doubling), but particularly because its occurrence is intrinsically caused by the discontinuous nature of the underlying system.

We first rewrite (2) in polar coordinates as

$$\begin{aligned} \dot{\rho} &= \rho\left(c(1-g_\epsilon(z)) - a g_\epsilon(z)\right) \\ \dot{\theta} &= -d(1-g_\epsilon(z)) - b g_\epsilon(z) \\ \text{where } z &= \rho\sin(\theta) - 1\ , \end{aligned} \tag{10}$$

and then (since $\dot{\theta} < 0$) we consider the following scalar equation

$$\frac{d\rho}{d\theta} = f(\rho,\theta) = \frac{(c(1-g_\epsilon(z)) - a g_\epsilon(z))}{(-d(1-g_\epsilon(z)) - b g_\epsilon(z))}\rho, \quad z = \rho\sin(\theta) - 1. \tag{11}$$

The existence of a limit cycle for (2) ensures the existence of a periodic solution of period 2π for (11). Now, let $N > 0$, N integer, take $\Delta = \frac{2\pi}{N}$ and denote with ϕ_Δ^ϵ the map obtained applying Euler's method with stepsize Δ to (11). Our aim is to give numerical evidence that ϕ_Δ^ϵ undergoes a period doubling cascade as ϵ decreases. We reason as follows.

A periodic orbit of period p for ϕ_Δ^ϵ, p a positive integer, is detected solving the following $(pN+1)$-dimensional nonlinear system for $(\rho_0, \rho_1, \ldots, \rho_{pN+1})$

$$\begin{aligned} \rho_1 &= \rho_0 + \Delta f(\rho_0, \theta_0) \\ &\vdots \\ \rho_{pN} &= \rho_{pN-1} + \Delta f(\rho_{pN-1}, \theta_{pN-1}) \end{aligned} \tag{12}$$

with $\theta_i = i\Delta$, $i = 0, \ldots, pN$ (of course, modulus 2π). The system is closed by the relation $\rho_{pN} = \rho_0$. Upon recursively expressing ρ_{pN} in terms of the previous terms, up to ρ_0, quite clearly the entire process can be formulated as a scalar map

$$\rho_0^+ \ = \ \Psi_\Delta^\epsilon(\rho_0)\ . \tag{13}$$

We seek fixed points of this map, and at convergence we monitor the value of $\frac{\partial}{\partial\rho_0}\Psi_\Delta^\epsilon$: a value of -1 is taken as indication of a period doubling bifurcation.

In our implementation, we solve (11) clockwise in θ (i.e., for negative θ), in agreement with the sign of $\dot{\theta}$ in (10). We use Euler's method and stepsize Δ, and we check for convergence of $(\rho_{(kN)} - \rho_0)$ to zero, where k is a positive integer. If,

ϵ	Period	Ratio
0.00621151300	2	
0.005097818578	4	
0.00488819181	8	5.312749...
0.00482735428	16	3.4456818...
0.00481444430	32	4.7124418...
0.00481166749	64	4.6492126...
0.00481107261	128	4.66784898...
0.00481094519	256	4.668691...

TABLE 1. Period doubling bifurcation values for Example 7. $N = 512$.

for $\bar{k} > 0$, we have $(\rho_{(\bar{k}N)} - \rho_0) \to 0$, then we infer that Ψ^{ϵ}_{Δ} has a stable periodic orbit of period $\bar{k}$.

In practice, we use the explicit recursion (12) only to obtain reasonable initial guesses for Newton's method, which is then used directly to find the fixed point of the map Ψ^{ϵ}_{Δ}. The algorithm is completed by a bisection search on ϵ in order to find flip bifurcation values. We illustrate in the next example.

Example 7. In (1), we fix the values $m = 1$, and $a = b = d = 1$ and $c = 0.8$. We know that system (1) admits an asymptotically stable crossing limit cycle and, for $\epsilon > 0$ and sufficiently small, also (2) admits an asymptotically stable limit cycle.

In what follows, we fix the stepsize $\Delta = \frac{2\pi}{512}$ unless otherwise specified, and we vary ϵ in order to detect bifurcation values. The results we obtain are summarized in Table 1.

Denote with ϵ_k, $k = 1, 2, \ldots$, the parameter values so that the fixed point ρ_0 of the 2^{k-1}st iterate of the map (13) undergoes a flip bifurcation (this betrays a bifurcating periodic orbit of twice the period for (12)). In the last column of Table 1, we report the ratios $\frac{\epsilon_k - \epsilon_{k-1}}{\epsilon_{k+1} - \epsilon_k}$, for $k = 2, \ldots, 7$. Quite clearly, these values are getting closer and closer to the Feigenbaum constant $\delta \simeq 4.6692$.

In Figure 3 we plot a zoom-in (otherwise, they are not distinguishable on this scale) of the asymptotically stable periodic orbit of period $2N$ and the unstable periodic orbit of period N for $\epsilon = 0.0055$. The limit cycle of period $2N$, in black, is approximated by solving (11) backward in θ with Euler's method and fixed stepsize $\Delta = \frac{2\pi}{512}$. We stop integrating when numerical convergence of $(\rho_{2N} - \rho_0)$ to 0 is reached. The unstable periodic orbit, in red, is obtained using Newton's method to solve (12) with $p = 1$.

Remark 8. When we change N from 512 to 513, qualitatively we obtain the same results as those reported above. However, there are quantitative differences. For example, the first period doubling (cfr. with Table 1) occurs at $\epsilon \approx 0.008138977285$.

In Figure 4 we plot in black the approximation of the limit cycle of (11) for $\epsilon = 0.0065$, obtained with the Matlab solver `ode45` (and error tolerances 10^{-10}). We contrast this result with those of the Euler method discretization of (11). In blue and red we plot the periodic orbit of period respectively N and $2N$ obtained applying Euler's method to (11) with stepsizes $\Delta = \frac{2\pi}{512}$ and $\Delta = \frac{2\pi}{256}$. In the latter case of Δ, the period doubling still occurs, but for larger values of ϵ. [As an example, the first bifurcation value for $N = 256$ is $\epsilon \simeq 0.016092612976$. Similarly, for larger values of N, the first bifurcation value occurs at smaller values of ϵ; e.g., with $N = 2^{10}$, we find $\epsilon \simeq 0.003793886115$.]

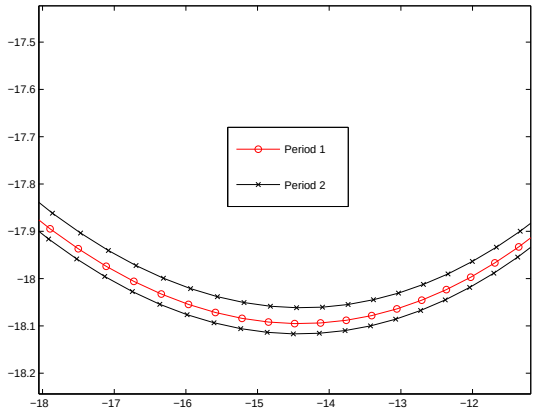

FIGURE 3. Example 7. Blow-up of the asymptotically stable periodic orbit of period $2N$ and unstable periodic orbit of period N for $\epsilon = 0.0055$.

The next two computations motivated us to analyze Euler method with event search, which we do in section 2.

(i) When we integrate (11) with the variable stepsize integrator `ODE45` from `Matlab` (and error tolerances of 10^{-10}), for ϵ as small as $\epsilon = 5 \times 10^{-16}$ we always obtain an invariant curve, which for small values of ϵ is indistinguishable from the limit cycle of the original discontinuous system. We believe that the reason for this success lies in the fact that the adaptive integration reduces the stepsize to the point of effectively forcing the method to step exactly on the discontinuity line; see our analysis of Euler method with event search in section 2.

(ii) If we convert (2) to *shifted polar coordinates*:

$$x_1 = r\cos(\theta),\ x_2 - 1 = r\sin(\theta), \tag{14}$$

we obtain (similarly to before) a scalar DE of the type $\frac{dr}{d\theta} = F(r,\theta)$. On this problem, repeating the experiments that led us to find period doubling in ϵ for fixed N relative to (11), we do not find any evidence of period doubling, at least none occurred for $N = 512$ and $\epsilon \geq 10^{-6}$. Again, we believe that this is due to the fact that –in these new variables, and for even N– we are forcing the method to step exactly on the discontinuity line, in a similar way to what an event-driven technique would do on the original discontinuous problem. As we will show in section 2, in this case the numerical method is able to accurately approximate the limit cycle.

To conclude the present sets of numerical experiments, we made one more computation, aimed at dispelling the suspicion that the observed period doubling is due to an artifact of fixing the initial angle at 0.

- Rather than discretizing (11) with $N = 512$ and $\Delta = 2\pi/N$, starting with $\theta_0 = 0$, of course one could discretize starting with a different θ_0. When we take $\theta_0 = k\Delta$ ($k = 1,\ldots,5$, for example), of course we recover the very same period doubling values of ϵ as with $\theta_0 = 0$. When we took $\theta_0 = \frac{k}{M}\Delta$, for $k = 1,\ldots,5$, and $M = 6$, again we obtained exactly (to 13 digits) the

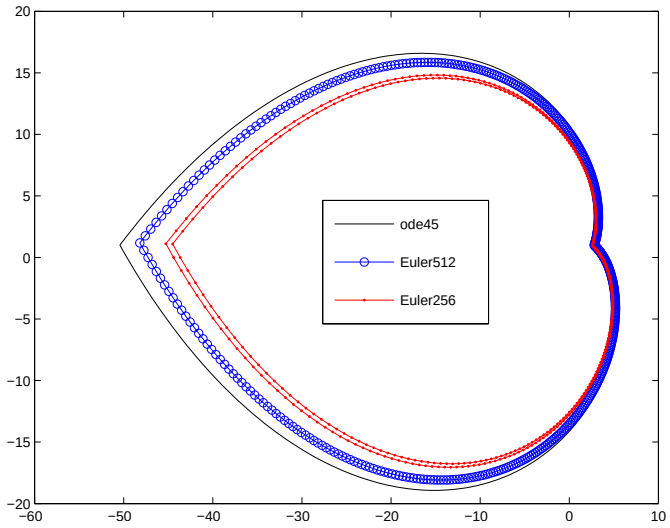

FIGURE 4. Example 7. Plot of the periodic orbit obtained with Euler's method versus the solution obtained with `ode45`; $\epsilon = 0.0065$.

same period doubling values once more. This confirms that the origin of the discretization has no impact on what we observed and reported in Table 1.

Based on the above numerical study, we formulate the following conjecture, relative to our model problem with $m = 1$, $a = b = d = 1$ and $c = 0.8$

Conjecture 3. *For any bounded N and any θ_0 and discretization points $\theta_k = \theta_0 + \frac{2\pi}{N}k$, $k = 1, \ldots, N$, there exists $\epsilon(N) > 0$ such that (13) has a period doubling bifurcation at $\epsilon(N) > 0$.*

We only have numerical evidence in support of Conjecture 3, numerical evidence based on using Newton's method. Instead, the following Fact holds as a consequence of Theorem 14 in Section 2.

Fact 4. *If we consider the map obtained when using the shifted polar variables (14), then, for any sufficiently large and even N, and $\epsilon > 0$, the map has no period doubling bifurcation.*

2. **Euler map with event location.** In this section we consider Forward Euler's method with event location (FWEL) applied to our discontinuous system (1), rewritten here in more compact form

$$\begin{bmatrix} \dot{x} \\ \dot{y} \end{bmatrix} = \begin{cases} f^-(x,y), & h(x,y) < 0 \\ f^+(x,y), & h(x,y) > 0 \end{cases}, \tag{15}$$

where f^- and f^+ are our linear problems in (1), $h(x,y) = y - m$, and we let $\Sigma = \{(x,y) \in \mathbb{R}^2 | h = 0\}$. We know that for $\frac{a}{b} > \frac{c}{d} > \frac{c_0}{d_0}$ [1], (15) has a crossing periodic orbit γ that intersects Σ in just two isolated points: $\bar{w}^- = (\bar{x}^-, m)$ and

[1] $\frac{c_0}{d_0}$ is a bifurcation value so that (1) has a crossing and sliding periodic orbit for $\frac{c}{d} < \frac{c_0}{d_0}$

$\bar{w}^+ = (\bar{x}^+, m)$ with $\bar{x}^- > 0 > \bar{x}^+$. We observe that for our problem, $\nabla h = \begin{bmatrix} 0 \\ 1 \end{bmatrix}$ and $(\nabla h)^T f^{\pm}(\bar{x}^-, m) < 0$ and $(\nabla h)^T f^{\pm}(\bar{x}^+, m) > 0$.

In what follows, we show that, for sufficiently small stepsize τ, FWEL applied to (15) has an attractive periodic orbit, close to that of the original problem. We show this result in two-stages: first, we show that there is a fixed point of a suitable Poincarè map, then we show that the fixed point is asymptotically stable.

The following notation will be handy:

$$\Sigma^+ = \{w \in \Sigma | \nabla h(w)^T f_{\pm}(w) > 0\} \ , \ \ \Sigma^- = \{w \in \Sigma | \nabla h(w)^T f_{\pm}(w) < 0\} \ .$$

To set the stage, we consider a fixed stepsize τ and we take an initial condition $\begin{bmatrix} x_0 \\ m \end{bmatrix} \in \Sigma^-$, with x_0 close to $\bar{x}^-$. Let $w = \begin{bmatrix} x \\ y \end{bmatrix}$, so that $w_0 = \begin{bmatrix} x_0 \\ m \end{bmatrix}$ and $h(w_0) = 0$.

Algorithm 2.1: FWEL: Forward Euler with Event Location

(i) Starting at w_0, compute the values $w_{n+1} = w_n + \tau f^-(w_n)$.

(ii) Let $k_1 = k_1(w_0) \in \mathbb{N}$ be the first index for which $h(w_{k_1+1}) > 0$ and consider the continuous extension $w_{k_1+1}(\delta) = w_{k_1} + \delta f^-(w_{k_1})$, $0 \le \delta \le \tau$.

(iii) Locate exactly $0 \le \tau(x_0) < \tau$ such that for $\delta = \tau(x_0)$, we have $h(w_{k_1+1}(\tau(x_0))) = 0$. Check that the transversality condition $\nabla h(w_{k_1+1}(\tau(x_0)))^T f^{\pm}(w_{k_1+1}(\tau(x_0))) > 0$ is satisfied[2].

(iv) Resume forward Euler steps from $\widehat{w}_0 = w_{k_1+1}(\tau(x_0))$.

(v) Let $k_2 = k_2(w_0) \in \mathbb{N}$ be the first index for which $h(w_{k_2+k_1+1}) > 0$ and consider the continuous extension $w_{k_2+k_1+1}(\delta) = w_{k_2+k_1} + \delta f^+(w_{k_2+k_1})$, $0 \le \delta \le \tau$.

(vi) Locate exactly $0 \le \tau(\widehat{x}_0) < \tau$ such that $h(w_{k_2+k_1+1}(\tau(\widehat{x}_0))) = 0$ and verify that the transversality condition $\nabla h(w_{k_2+k_1+1}(\tau(\widehat{x}_0)))^T f^{\pm}(w_{k_2+k_1+1}(\tau(\widehat{x}_0))) > 0$ is satisfied.

(vii) Go back to (i), with $w_0 = w_{k_2+k_1+1}(\tau(\widehat{x}_0))$.

As already noticed in Algorithm 2.1-(iii), there is a neighborhood $I_{\bar{w}^-}$ of $\bar{w}^-$, such that, for all $x_0 \in I_{\bar{w}^-} \cap \Sigma^- = I_{\bar{x}^-}$, the corresponding $w_{k_1+1}(\tau(x_0))$ is in Σ^+ (i.e. not in the sliding segment) for τ sufficiently small. Now, consider the map $P_\tau^- : I_{\bar{x}^-} \to \Sigma^+$ defined as follows. $P_\tau^-(w)$ is the point $w_{k_1+1}(\tau(x_0))$ on Σ obtained performing steps (i)-(iii) above with $w_0 = w$. This map is continuous and Lipschitz with respect to x as we will prove in Lemma 9 below.

Lemma 9. *The map P_τ^- is continuous and Lipschitz with respect to x in $I_{\bar{x}^-}$.*

Proof. We use the same notation as in steps (i)-(iii) above. It is obvious that w_n in (i) is smooth with respect to x_0. We still need to show that $w_{k_1+1}(\tau(x_0))$ and hence $\tau(x_0)$ in (iii) is Lipschitz with respect to x_0. We consider two cases.

[$\tau(x_0) > 0$] Consider the map $M : I \times \mathbb{R}^2 \to \mathbb{R}$ defined as $M(\delta, w) = h(\omega + \delta f^-(\omega))$. Notice that $M(\tau(x_0), w_{k_1}) = 0$ and $\frac{\partial M}{\partial \delta}|_{(\tau(x_0), w_{k_1})} = \nabla h(w_{k_1+1}(\tau(x_0)))^T$

$f^-(w_{k_1}) \neq 0$, for $\tau(x_0)$ (and hence τ) sufficiently small and x_0 sufficiently close to $\bar{x}^-$. Then, by the implicit function theorem, there exists a neighborhood of $\tau(x_0)$, $I_{\tau(x_0)}$, a neighborhood of w_{k_1}, $I_{w_{k_1}}$, and a smooth function $\delta : I_{w_{k_1}} \to I_{\tau(x_0)}$, such that $M(\delta(w), w) = 0$. This means that, for each $x_0 \in I^-_{\bar{x}}$ and such that $h(w_{k_1+1}) > 0$, $\tau(x_0)$ is a smooth function of x_0 and so is P^-_τ.

$[\tau(x_0) = 0\ ]$ We make explicit the dependence on the initial condition x_0 of the quantities introduced in (i)-(iii): $x_n = x_n(x_0)$, etc.. The point (x_0, m) is such that $h(w_{k_1}(x_0)) = 0$ so that $w_{k_1+1}(\tau(x_0)) = w_{k_1}(x_0)$. Then in any neighborhood I_{x_0} of (x_0, m) there are points $x \in I_{x_0} \cap \Sigma^-$ such that $h(w_{k_1}(x)) < 0$, and points $x \in I_{x_0} \cap \Sigma^-$ such that $h(w_{k_1}(x)) > 0$. In the latter case, instead of the continuous extension $w_{k_1+1}(\delta(x))$ in (ii), we need to consider the continuos extension $w_{k_1}(\delta(x))$. Let M be the map defined for the case $[\tau(x_0) > 0]$ and notice that $M(0, w_{k_1}(x_0)) = M(\tau, w_{k_1-1}(x_0)) = 0$. Moreover for τ sufficiently small $\frac{\partial M}{\partial \delta}|_{(0,w_{k_1}(x_0))} \neq 0$, and $\frac{\partial M}{\partial \delta}|_{(\tau,w_{k_1-1}(x_0))} \neq 0$. Then there are a neighborhood of $w_{k_1}(x_0)$, $I_{w_{k_1}(x_0)}$, a neighborhood of 0, I_0, and a smooth function $\delta_1 : I_{w_{k_1}(x_0)} \to I_0$ such that $M(\delta_1(w), w) = 0$. Similarly, there are a neighborhood of $w_{k_1-1}(x_0)$, $I_{w_{k_1-1}(x_0)}$, a neighborhood of τ, I_τ, and a smooth function $\delta_2 : I_{w_{k_1-1}(x_0)} \to I_\tau$, such that $M(\delta_2(w), w) = 0$. Notice that $\delta_1(w_{k_1}(x_0)) = 0$, $\delta_2(w_{k_1-1}(x_0)) = \tau$ and the two continuous extensions $w_{k_1+1}(\delta)$ and $w_{k_1}(\delta)$ satisfy the following: $w_{k_1+1}(\delta_1(w_{k_1}(x_0))) = w_{k_1}(\delta_2(w_{k_1-1}(x_0))) = w_{k_1}$. For x in a neighborhood of x_0 and $w_0 = (x, m)$, we define the following function

$$w_l(\delta(w)) = \begin{cases} w_{k_1+1}(\delta_1(w)) & h(w_{k_1+1}(x)) > 0,\ \ h(w_{k_1}(x)) \leq 0 \\ w_{k_1}(\delta_2(w)) & h(w_{k_1}(x)) > 0,\ \ h(w_{k_1-1}(x)) \leq 0 \end{cases}$$

and this function is Lipschitz and not differentiable at the point $x = x_0$.

□

Similarly to P^-_τ, we define the map $P^+_\tau : \Sigma^+ \to \Sigma^-$ that associates to each point on Σ^+, the point on Σ^- obtained performing steps (iv)-(vi) above with starting point $w = w_{k_1+1}(\bar{\delta})$. This map is well defined in a neighborhood of $\bar{x}^+$ and it is continuous and Lipschitz with respect to x. The proof is similar to the proof of Lemma 9. The composite map $P_\tau : \Sigma^- \to \Sigma^-$, $P_\tau = P^+_\tau \circ P^-_\tau$ is then well defined in $I_{\bar{x}^-}$ and is continuous with respect to x.

In what follows, we denote with $\overline{I_{\bar{x}^-}}$ the closure of the set $I_{\bar{x}^-}$.

Lemma 10. *The set $\overline{I_{\bar{x}^-}}$ is invariant under P_τ, for τ sufficiently small.*

Proof. Let P denote the Poincaré map of the continuous problem. Then, since γ is globally asymptotically stable, $P(\overline{I_{\bar{x}^-}})$ is a proper subset of $\overline{I_{\bar{x}^-}}$ and it is closed. Let $d = \beta(P(\overline{I_{\bar{x}^-}}), \overline{I_{\bar{x}^-}})$, with $\beta(A, B) = \min_{b \in B} \rho(A, b)$ and $\rho(A, b)$ distance of the point b from the set A. Then d is bounded away from 0. The statement of the lemma follows upon noticing that the global error for FWEL is $O(\tau)$ (e.g., see [5]). Then, for τ sufficiently small, $\text{dist}(P(\overline{I_{\bar{x}^-}}), P_\tau(\overline{I_{\bar{x}^-}})) < \frac{d}{2}$, so that $P_\tau(\overline{I_{\bar{x}^-}}) \subset \overline{I_{\bar{x}^-}}$. Then $\overline{I_{\bar{x}^-}}$ is invariant under P_τ. □

Using Lemma 9 and 10, we can prove the following.

Proposition 11. *There exists $\bar{\tau} > 0$, such that, for all $\tau < \bar{\tau}$, and bounded away from 0, FWEL has a periodic orbit γ_τ in a neighborhood of γ.*

Proof. We apply Brouwer's fixed point Theorem to the map P_τ. Then P_τ has a fixed point, denote it with $(\bar{x}_\tau^-, m)$. Moreover, let $\bar{w}_\tau^- = (\bar{x}_\tau^-, m)$ and consider $w_1 = \bar{w}_\tau^- + \tau f^-(\bar{w}_\tau^-)$. Since $f^-(\bar{w}_\tau^-) \neq 0$, then $w_1 \neq \bar{w}_\tau^-$ and $\bar{w}_\tau^-$ is not a spurious fixed point of FWEL. □

Next, we will show that γ_τ is attractive. Let $(\bar{x}_\tau^-, m)$ and $(\bar{x}_\tau^+, m)$ be the two intersection points of γ_τ respectively with Σ^- and Σ^+, $\bar{x}_\tau^- > \bar{x}_\tau^+$. Moreover, for τ sufficiently small, the following inequalities must be satisfied

$$\bar{x}_\tau^- > \frac{c}{d}m, \;\; \bar{x}_\tau^+ < -\frac{a}{b}m. \tag{16}$$

Let $\bar{w}_0^- = (\bar{x}_\tau^-, m)^T$ and denote with $\bar{w}_k$ the k-th iterate of FWEL with initial condition $\bar{w}_0^-$. Let $N_1(\bar{w}_0^-)$ be such that $h(\bar{w}_{N_1(\bar{w}_0^-)+1}) > m$ and let $\tau^-(\bar{x}_\tau^-)$ be defined as in step (iii) of Algorithm 2.1. Then

$$\begin{bmatrix} \bar{x}_\tau^+ \\ m \end{bmatrix} = S_-(\tau^-(\bar{x}_\tau^-))S_-(\tau)^{N_1(\bar{w}_0^-)} \begin{bmatrix} \bar{x}_\tau^- \\ m \end{bmatrix}, \tag{17}$$

with $S_-(t) = \begin{pmatrix} 1+tc & td \\ -td & 1+tc \end{pmatrix}$. Let $\bar{w}_0^+ = (\bar{x}_\tau^+, m)^T$ and denote with $\bar{w}_k^+$ the k-th iterate of FWE with initial condition $\bar{w}_0^+$. Let $N_2(\bar{w}_0^+)$ be such that $h(\bar{w}^+_{N_2(\bar{w}_0^+)+1}) < m$ and let $\tau^+(\bar{x}_\tau^+)$ be defined as in step (vi) of Algorithm 2.1. Then

$$\begin{bmatrix} \bar{x}_\tau^- \\ m \end{bmatrix} = S_+(\tau^+(\bar{x}_\tau^+))S_+(\tau)^{N_2(\bar{w}_0^+)} \begin{bmatrix} \bar{x}_\tau^+ \\ m \end{bmatrix}, \tag{18}$$

with $S_+(t) = \begin{bmatrix} 1-ta & tb \\ -tb & 1-ta \end{bmatrix}$.

More in general, given a vector $(x_0^-, m)^T$ in a neighborhood of $(\bar{x}_\tau^-, m)^T$, we denote with (x_0^+, m) the intersection point with Σ^+ of the FWEL sequence with initial point $(x_0^-, m)^T$. Let $\tau(x_0^-)$ and $\tau(x_0^+)$ be the intermediate stepsizes as defined in (iii) and (vi) of Algorithm 2.1, respectively. Then, the transition matrix $S(\tau, x_0^-)$ of FWEL that takes $(x_0^-, m)^T$ back to Σ^- is the following

$$\begin{aligned} S(\tau, x_0^-) &= S_+(\tau(x_0^+))S_+(\tau)^{N_2(x_0^+)}S_-(\tau(x_0^-))S_-(\tau)^{N_1(x_0^-)} \\ &= \begin{pmatrix} \mathrm{Re}(\lambda(\tau, x_0^-)) & \mathrm{Im}(\lambda(\tau, x_0^-)) \\ -\mathrm{Im}(\lambda(\tau, x_0^-)) & \mathrm{Re}(\lambda(\tau, x_0^-)) \end{pmatrix}, \end{aligned} \tag{19}$$

with

$$\lambda(\tau, x_0^-) = \lambda_+(\tau(x_0^+))\lambda_-(\tau(x_0^-))\lambda_+(\tau)^{N_2(x_0^+)}\lambda_-(\tau)^{N_1(x_0^-)}, \tag{20}$$

where $\lambda_-(t) = (1+tc) + i(td)$, $\lambda_+(t) = (1-ta) + i(tb)$. Notice that $S_-(t)$ equals to $|\lambda_-(t)|$ times a rotation matrix, with rotation angle $\varphi_-(t) = \arctan(\frac{dt}{1+ct})$. Then the transition matrix $S(\tau, x^-)$ is given by a rotation matrix times $|\lambda(\tau, x^-)|$. Similarly for $S_+(t)$. Moreover for $x^- = \bar{x}_\tau^-$, it must be $\lambda(\tau, \bar{x}_\tau^-) = 1$ and $S(\tau, \bar{x}_\tau^-) = I$. Let now $(x_0^-, m)^T$ be a point in $I_{\bar{x}^-}$ and $(x_k^-, m) = P_\tau((x_{k-1}^-, m)) = P_\tau^k((x_0^-, m))$. E.g., for $k = 1$, $(x_1^-, m) = S(\tau, x_0^-)(x_0^-, m)^T$.

In order to show attractivity of γ_τ, we will show that, for $x_0^- > \bar{x}_\tau^-$ (resp. $x_0^- < \bar{x}_\tau^-$), we have $\bar{x}_\tau^- < x_1^- < x_0^-$ (resp. $\bar{x}_\tau^- > x_1^- > x_0^-$). In this way the sequence $\{x_k^-\}$ is monotone decreasing (resp. increasing) and bounded from below (resp. above) and it hence must converge to a point $\bar{x}$. Since it must be $(\bar{x}, m) = \lim_{k\to\infty}(x_k^-, m) = \lim_{k\to\infty} P_\tau((x_{k-1}^-, m)) = P((\bar{x}, m))$, then $\bar{x} = \bar{x}_\tau^-$. We will show the following steps

(a) Let $x_0^- > \bar{x}_\tau^-$ (resp. $x_0^- < \bar{x}_\tau^-$). Then $x_0^+ < \bar{x}_\tau^+$ (resp. $x_0^+ > \bar{x}_\tau^+$).
(b) If $x_0^- > \bar{x}_\tau^-$ (resp. $x_0^- < \bar{x}_\tau^-$) then $N_1(x_0^-) \le N_1(\bar{x}_\tau^-)$ (resp. $N_1(x_0^-) \ge N_1(\bar{x}_\tau^-)$).
(c) If $x_0^- > \bar{x}_\tau^-$ (resp. $x_0^- < \bar{x}_\tau^-$) and $N_1(x_0^-) = N_1(\bar{x}_\tau^-)$ then $\tau(x_0^-) < \tau(\bar{x}_\tau^-)$ (resp. $\tau(x_0^-) > \tau(\bar{x}_\tau^-)$).

Then, reasoning in a similar way, the next three steps can be proven as well.

(d) Let $x_0^+ < \bar{x}_\tau^+$ (resp. $x_0^+ > \bar{x}_\tau^+$). Then $x_1^- > \bar{x}_\tau^-$ (resp. $x_1^- < \bar{x}_\tau^+$).
(e) If $x_0^+ < \bar{x}_\tau^+$ (resp. $x_0^+ > \bar{x}_\tau^+$) then $N_2(x_0^+) \ge N_2(\bar{x}_\tau^+)$ (resp. $N_2(x_0^+) \le N_2(\bar{x}_\tau^+)$).
(f) If $x_0^+ < \bar{x}_\tau^+$ (resp. $x_0^+ > \bar{x}_\tau^-$) and $N_2(x_0^+) = N_2(\bar{x}_\tau^+)$ then $\tau(x_0^+) > \tau(\bar{x}_\tau^+)$ (resp. $\tau(x_0^+) < \tau(\bar{x}_\tau^+)$).

For $x_0^- > \bar{x}_\tau^-$, (b) and (c) above imply that $\lambda_-(\tau(x_0^-))\lambda_-(\tau)^{N_1(x_0^-)} > \lambda_-(\tau(\bar{x}_\tau^-))$ $\lambda_-(\tau)^{N_1(\bar{x}_\tau^-)}$, while items (e) and (f) imply that $\lambda_+(\tau(x_0^+))\lambda_+(\tau)^{N_2(x_0^+)} < \lambda_+(\tau(\bar{x}_\tau^+))$ $\lambda_+(\tau)^{N_2(\bar{x}_\tau^+)}$. It follows that, for $x_0^- > \bar{x}_\tau^-$, $\lambda(\tau, x_0^-)$ in (20) must be less than 1 and hence $x_1^- < x_0^-$. Moreover items (a) and (d) imply $x_1^- > \bar{x}_\tau^-$ so that the claim is proven.

The following Lemma suffices to show (a) above.

Lemma 12. *Let (x_0, m) and $(\widehat{x}_0, m)$ be such that $x_0, \widehat{x}_0 > \frac{c}{d}m$, $\tau > 0$ and consider the Euler trajectories given by the points $\begin{bmatrix} x_k \\ y_k \end{bmatrix} = S_-(\tau)^k \begin{bmatrix} x_0 \\ m \end{bmatrix}$ and $\begin{bmatrix} \widehat{x}_k \\ \widehat{y}_k \end{bmatrix} = S_-(\tau)^k \begin{bmatrix} \widehat{x}_0 \\ m \end{bmatrix}$, $k = 0, \dots, N+1$. Then, the line segments given by joining two consecutive points of each trajectory do not intersect.*

Proof. We have

$$\begin{bmatrix} x_k \\ y_k \end{bmatrix} = S_-(\tau)^k \begin{bmatrix} x_0 \\ m \end{bmatrix}, \text{ and } \begin{bmatrix} \widehat{x}_k \\ \widehat{y}_k \end{bmatrix} = S_-(\tau)^k \begin{bmatrix} \widehat{x} \\ m \end{bmatrix},$$

with $S_-(\eta) = \begin{bmatrix} 1+\eta c & \eta d \\ -\eta d & 1+\eta c \end{bmatrix} = |\lambda_-(\eta)| \begin{bmatrix} \cos(\varphi_-(\eta)) & \sin(\varphi_-(\eta)) \\ -\sin(\varphi_-(\eta)) & \cos(\varphi_-(\eta)) \end{bmatrix}$, $\lambda_-(\eta) = (1+\eta c) + i(\eta d)$, $\varphi(\eta) = \arctan \frac{\eta d}{1+\eta c}$. Therefore, if we let $L = \log(S_-(\tau))$, we are sampling at integer times the solutions of the linear system

$$\frac{d}{dt} \begin{bmatrix} x \\ y \end{bmatrix} = L \begin{bmatrix} x \\ y \end{bmatrix}, \text{with ICs } \begin{bmatrix} x_0 \\ m \end{bmatrix} \text{ or } \begin{bmatrix} \widehat{x}_0 \\ m \end{bmatrix}.$$

Now, since solutions of the differential equation cannot intersect, we know that the (continuous) trajectories $\begin{bmatrix} x(t) \\ y(t) \end{bmatrix} = e^{Lt} \begin{bmatrix} x_0 \\ m \end{bmatrix}$ and $\begin{bmatrix} \widehat{x}(t) \\ \widehat{y}(t) \end{bmatrix} = e^{Lt} \begin{bmatrix} \widehat{x}_0 \\ m \end{bmatrix}$ do not intersect. If $x_0 > \widehat{x}_0$, then $\begin{bmatrix} x(t) \\ y(t) \end{bmatrix}$ stays outside the trajectory $\begin{bmatrix} \widehat{x}(t) \\ \widehat{y}(t) \end{bmatrix}$. In particular, the points $\begin{bmatrix} x_k \\ y_k \end{bmatrix}$, and $\begin{bmatrix} \widehat{x}_k \\ \widehat{y}_k \end{bmatrix}$ are distinct, the former lying on the trajectory $\begin{bmatrix} x(t) \\ y(t) \end{bmatrix}$ and the latter on the trajectory $\begin{bmatrix} \widehat{x}(t) \\ \widehat{y}(t) \end{bmatrix}$. To verify the claim that the Euler segments do

not intersect, consider these line segments. With $0 \le s, \widehat{s} \le 1$, we have

$$\begin{bmatrix} x(s) \\ y(s) \end{bmatrix} = \begin{bmatrix} x_k \\ y_k \end{bmatrix} + s \begin{bmatrix} x_{k+1} - x_k \\ y_{k+1} - y_k \end{bmatrix} = S_-(s\tau) \begin{bmatrix} x_k \\ y_k \end{bmatrix}$$
$$\begin{bmatrix} \widehat{x}(\widehat{s}) \\ \widehat{y}(\widehat{s}) \end{bmatrix} = \begin{bmatrix} \widehat{x}_k \\ \widehat{y}_k \end{bmatrix} + \widehat{s} \begin{bmatrix} \widehat{x}_{k+1} - \widehat{x}_k \\ \widehat{y}_{k+1} - \widehat{y}_k \end{bmatrix} = S_-(\widehat{s}\tau) \begin{bmatrix} \widehat{x}_k \\ \widehat{y}_k \end{bmatrix}.$$

If these two segments intersect, there must be values of $s, \widehat{s}$: $0 < s, \widehat{s} < 1$ (since end points are distinct), where $\begin{bmatrix} x(s) \\ y(s) \end{bmatrix} = \begin{bmatrix} \widehat{x}(\widehat{s}) \\ \widehat{y}(\widehat{s}) \end{bmatrix}$ and this implies

$$\begin{bmatrix} x_k \\ y_k \end{bmatrix} = S_-(s\tau)^{-1} S_-(\widehat{s}\tau) \begin{bmatrix} \widehat{x}_k \\ \widehat{y}_k \end{bmatrix} = \frac{|\lambda_-(\widehat{s}\tau)|}{|\lambda_-(s\tau)|} \begin{bmatrix} \cos(\varphi) & \sin(\varphi) \\ -\sin(\varphi) & \cos(\varphi) \end{bmatrix} \begin{bmatrix} \widehat{x}_k \\ \widehat{y}_k \end{bmatrix}, \tag{21}$$

with $\varphi = \varphi_-(\widehat{s}\tau) - \varphi_-(s\tau)$. Now notice that, for $x_0 > \widehat{x}_0 > \frac{c}{d}m$, it must be $\left\| \begin{bmatrix} x_k \\ y_k \end{bmatrix} \right\| > \left\| \begin{bmatrix} \widehat{x}_k \\ \widehat{y}_k \end{bmatrix} \right\|$ and hence $s > \widehat{s}$ so that in (21) $\frac{|\lambda_-(\widehat{s}\tau)|}{|\lambda_-(s\tau)|} > 1$. At the same time $x_0 > \widehat{x}_0$ implies that the angle between $\begin{bmatrix} x_0 \\ m \end{bmatrix}$ and $\begin{bmatrix} \widehat{x}_0 \\ m \end{bmatrix}$ is negative, we denote it with θ. Now, θ must be equal to φ in (21), i.e. to the angle between $\begin{bmatrix} x_k \\ y_k \end{bmatrix}$ and $\begin{bmatrix} \widehat{x}_k \\ \widehat{y}_k \end{bmatrix}$. However $s > \widehat{s}$ implies that $\varphi = \varphi_-(\widehat{s}\tau) - \varphi_-(s\tau) > 0$. This is a contradiciton. □

To show (b), we use same notations as in the proof of Lemma 12. Let $x_0 > \widehat{x}_0$ and let $w = \begin{bmatrix} x_{N_1(\widehat{x}_0)+1} \\ y_{N_1(\widehat{x}_0)+1} \end{bmatrix}$ and $\widehat{w} = \begin{bmatrix} \widehat{x}_{N_1(\widehat{x}_0)} + 1 \\ \widehat{y}_{N_1(\widehat{x}_0)+1} \end{bmatrix}$. Then $\|w\| > \|\widehat{w}\|$ and moreover the angle between $\widehat{w}$ and w is negative so that w is above $\widehat{w}$. Then $\begin{bmatrix} x_{N_1(\widehat{x}_0)+1} \\ y_{N_1(\widehat{x}_0)+1} \end{bmatrix}$ is above $y = m$ and hence $N_1(x_0) \le N_1(\widehat{x}_0)$.

Finally (c) is proven in the following Lemma.

Lemma 13. *Let $x_0^- > \bar{x}_\tau^-$ and $N_1(x_0^-) = N_1(\bar{x}_\tau^-)$. Then $\tau(x_0^-) < \tau(\bar{x}_\tau^-)$.*

Proof. Let $S_-(\tau, x_0^-) = S(\tau(x_0^-))S(\tau)^{N_1(x_0^-)}$ (see (19)) and consider $w^+ = (x_0^+, m)^T = S_-(\tau, x_0^-)(x^-, m)^T$. Let $\bar{w} = S_-(\tau, x_0^-)(\bar{x}_\tau^-, m)^T$. Then $\bar{w}$ lies below w^+ and $\|\bar{w}\| < \|w^+\|$. It follows that $\bar{w}$ does not intersect Σ^+ and hence $\tau(\bar{x}_\tau^-) > \tau(x_0^-)$. □

Theorem 14. *There exists a $\bar{\tau} > 0$, so that, for all $\tau < \bar{\tau}$, and bounded away from 0, FWEL has an attractive periodic orbit γ_τ. Moreover*

$$\lim_{\tau \to 0} \bar{x}_\tau^- = \bar{x}^-.$$

Proof. Attractivity of γ_τ implies that γ_τ is an isolated periodic orbit. This together with $|P_\tau(\bar{x}^-) - \bar{x}^-| = O(\tau)$, implies convergence of $\bar{x}_\tau^-$ to $\bar{x}^-$. □

3. **The band. Proof of Claim 1.** In what follows let $w_k(\tau)$ be the k-th element of the FWE sequence with initial condition w_0 and with stepsize τ. We denote with $\gamma_{t,\tau}(w_0)$ the broken line approximation with nodes $w_k(\tau)$, $k \ge 0$. A point z of $\gamma_{t,\tau}(w)$ must satisfy the following: there exists $t \in [0, \tau)$ and $k \ge 0$ such that

$$z = \begin{cases} S_-(t)w_k(\tau), & \text{if } h(w_k(\tau)) < m \text{ or } w_k(\tau) \in \Sigma^- \\ S_+(t)w_k(\tau) & \text{if } h(w_k(\tau)) > m \text{ or } w_k(\tau) \in \Sigma^+ \end{cases},$$

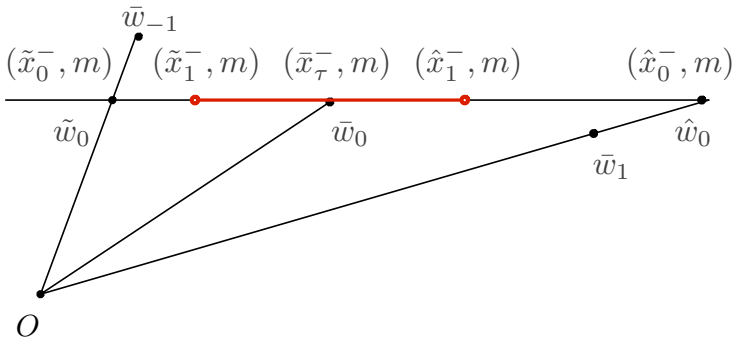

FIGURE 5. In support of the proof of Claim 1. The red segment contains the band.

with $S_-(t) = \begin{pmatrix} 1+tc & td \\ -td & 1+tc \end{pmatrix}$ and $S_+(t) = \begin{pmatrix} 1-ta & td \\ -td & 1-ta \end{pmatrix}$. Take $w_0 = (x_0, m) \in \Sigma^-$ and consider the broken line interpolant $\gamma_{t,\tau}(w_0)$.

Denote with $\bar{w}_0^- = (\bar{x}_\tau^-, m)^T$ and $\bar{w}_0^+ = (\bar{x}_\tau^+, m)^T$ the intersection points of γ_τ with Σ^- and Σ^+ respectively, where γ_τ is the periodic orbit of FWEL as described in Section 2. Consider one Euler step with initial condition $\bar{w}_0 = \bar{w}_0^-$ and stepsize τ: $\bar{w}_1 = S_-(\tau)(\bar{x}_\tau^-, m)^T$. Then

$$\bar{w}_1 = \begin{pmatrix} \bar{x}_\tau^- + \tau(c\bar{x}_\tau^- + dm) \\ m + \tau(-d\bar{x}_\tau^- + cm) \end{pmatrix},$$

and for τ sufficiently small and $\bar{x}_\tau^- > \frac{c}{d}m$ (see (16)), the second component of $\bar{w}_1$ satisfies the following inequality: $0 < e_2^T \bar{w}_1 < m$. Then we can prolong $\bar{w}_1$ until it intersects Σ^- and we denote this intersection point as $\widehat{w}_0 = (\widehat{x}_0^-, m)^T$, see Figure 5. Then $\widehat{w}_0 = \alpha \bar{w}_1$, where α is such that $e_2^T \widehat{w}_0 = m$, i.e.,

$$\alpha = \frac{m}{m + \tau(mc - d\bar{x}_\tau^-)} > 1, \tag{22}$$

because $\bar{x}_\tau^- > \frac{c}{d}m$.

The following inequalities are satisfied: $\|\widehat{w}_0\| > \|\bar{w}_1\|$ and $\widehat{x}_0^- > \bar{x}_\tau^-$. See Figure 5.

Moreover, since $\widehat{x}_0^- = m\frac{\bar{x}_\tau^- + \tau(c\bar{x}_\tau^- + dm)}{m + \tau(-d\bar{x}_\tau^- + cm)}$, then

$$\widehat{x}_0^- - \bar{x}_\tau^- = \tau \frac{md\left((\bar{x}_\tau^-)^2 + m\right)}{m + \tau(-d\bar{x}_\tau^- + cm)} = O(\tau)\ . \tag{23}$$

Consider the Euler iterates $\widehat{w}_k$ with initial condition $\widehat{w}_0$ and stepsize τ and take the broken line approximation $\gamma_{t,\tau}(\widehat{w}_0)$ with nodes $\widehat{w}_k$, $k \geq 0$. Then $\gamma_{t,\tau}(\widehat{w}_0)$ meets Σ^+ at a point that we denote as $(\widehat{x}_0^+, m)^T$, it crosses Σ^+ and it meets Σ^- again at a point $(\widehat{x}_1^-, m)$.

In a similar way, we consider the vector $\bar{w}_{-1} = S_-(\tau)^{-1}\bar{w}^-$. We denote with $\widetilde{w}_0 = (\widetilde{x}_0^-, m)^T$ the intersection point of $\widetilde{w}_{-1}$ with Σ^-. Then $\|\widetilde{w}_0\| < \|\bar{w}_{-1}\|$, see Figure

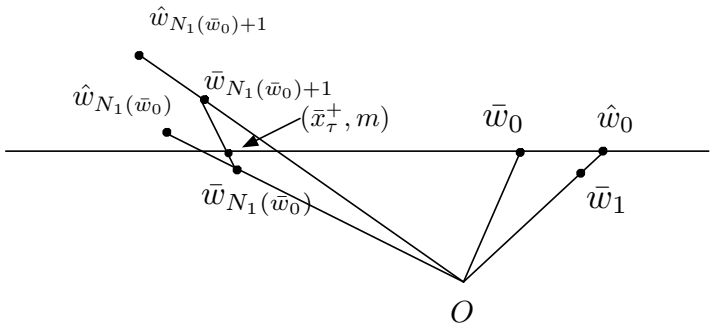

FIGURE 6. In support of Lemma 15

5, and $\widetilde{x}_0^- < \bar{x}_\tau^-$, and $\widetilde{x}_0^- > 0$ for small τ. Moreover, since $\widetilde{x}_0^- = m\frac{\bar{x}_\tau^- + \tau(c\bar{x}_\tau^- - dm)}{m+\tau(d\bar{x}_\tau^- + cm)}$, then

$$\bar{x}_\tau^- - \widetilde{x}_0^- = \tau \frac{d\left((\bar{x}_\tau^-)^2 + m^2\right)}{m + \tau(d\bar{x}_\tau^- + cm)} = O(\tau)\ .$$

We consider the Euler iterates $\widetilde{w}_k$ with initial condition $\widetilde{w}_0$ and stepsize τ together with the broken line approximation $\gamma_{t,\tau}(\widetilde{w}_0)$ with nodes $\widetilde{w}_k$. Then $\gamma_{t,\tau}(\widetilde{w}_0)$ meets Σ^+ at $(\widetilde{x}_0^+, m)^T$, it crosses it, and meets Σ^- again at $(\widetilde{x}_1^-, m)^T$.

Lemma 15. *With the above notation, for τ sufficiently small, it holds*

$$\widehat{x}_1^- < \widehat{x}_0^-,\ \ \widetilde{x}_1^- > \widetilde{x}_0^-.$$

Proof. We will show that $\|(\widehat{x}_1^-, m)\| < \|\widehat{x}_0^-, m\|$ and this implies $\widehat{x}_1^- < \widehat{x}_0^-$. The argument to show $\widetilde{x}_1^- > \widetilde{x}_0^-$ is much the same.

We will use the following notation. For a $z_0 \in \Sigma^-$, let z_k, $k \in \mathbb{N}$ be the k-th element of the sequence generated by FWE and denote with $N_1(z_0)$ the first iterate number such that $e_2^T z_{N_1(z_0)+1} > m$ and with $N_2(z_0)$ the first iterate number such that $e_2^T z_{N_1(z_0)+1+N_2(z_0)+1} < m$.

Consider the broken line approximation $\gamma_{t,\tau}(z_0)$. Then, for $z_0 = (x_0^-, m)^T$ close to $\bar{w}_0$, $\gamma_{t,\tau}(z_0)$ intersects Σ^- between the iterates $z_{N_1(z_0)+1+N_2(z_0)}$ and $z_{N_1(z_0)+1+N_2(z_0)+1}$ at $(x_1^-, m)^T$. We have the following expression

$$\begin{bmatrix} x_1^- \\ m \end{bmatrix} = S_+(\tau^+(z_0))S_+(\tau)^{N_2(z_0)}S_-(\tau)^{N_1(z_0)+1}z_0. \tag{24}$$

For $z = \bar{w}_0$, let $e_2^T\bar{w}_{N_1(\bar{w}_0)+1} \geq m$ and notice that $e_2^T\widehat{w}_{N_1(\bar{w}_0)} > m$, since $\widehat{w}_{N_1(\bar{w}_0)} = \alpha\bar{w}_{N_1(\bar{w}_0)+1}$, with $\alpha > 1$ as in (22), see Figure 6.

It follows that $N_1(\widehat{w}_0) \leq N_1(\bar{w}_0) - 1$, and this implies

$$|\lambda_-(\tau)|^{N_1(\widehat{w}_0)+1} < |\lambda_-(\tau(\bar{w}))||\lambda_-(\tau)|^{N_1(\bar{w}_0)}, \tag{25}$$

with $\lambda_-(\eta) = (1+\eta c)+i\eta d$ and with $\tau(\bar{w})$ being the intermediate stepsize as defined in Algorithm 2.1, (iii).

Notice moreover that it must be $N_1(\widehat{w}_0) \geq N_1(\bar{w}_0) - 2$. Indeed, assume by contradiction that $N_1(\widehat{w}_0) = N_1(\bar{w}_0) - 3$. Then we must have $e_2^T \widehat{w}_{N_1(\bar{w}_0)-2} = \alpha e_2^T \bar{w}_{N_1(\bar{w}_0)-1} > m$, with α as in (22). At the same time, $e_2^T \bar{w}_{N_1(\bar{w}_0)} < m$ together with $\bar{w}_{N_1(\bar{w}_0)} = S_-(\tau)\bar{w}_{N_1(\bar{w}_0)-1}$, implies

$$\begin{aligned}\alpha(e_2^T \bar{w}_{N_1(\bar{w}_0)-1}) <& \frac{m}{m+\tau(cm-d\bar{x}_\tau^-)} \frac{m+\tau d(e_1^T \bar{w}_{N_1(\bar{w}_0)-1})}{1+\tau c} \\ =& \frac{m}{1+\tau c} \frac{m+\tau d(e_1^T \bar{w}_{N_1(\bar{w}_0)-1})}{m+\tau(cm-d\bar{x}_\tau^-)}. \end{aligned} \tag{26}$$

Now, if we show that $\tau d(e_1^T \bar{w}_{N_1(\bar{w}_0)} - 1) < \tau(cm - d\bar{x}_\tau^-)$, then we have that $\alpha(e_2^T \bar{w}_{N_1(\bar{w}_0)-1}) < m$ and hence a contradiction. To this end we just notice that, for τ sufficiently small, $d(e_1^T \bar{w}_{N_1(\bar{w}_0)-1})$ is close to $d\bar{x}_\tau^+$ and $\tau(d\bar{x}_\tau^+ + d\bar{x}_\tau^-) < 0 < \tau cm$.

Next, we move $\widehat{w}_{N_1(\widehat{w}_0)+1}$ forward by the same map used in (18) and we get a new vector

$$\widehat{z} = S_+(\tau^+(\bar{x}_\tau^+))S_+(\tau)^{N_2(\bar{w}_0^+)}\widehat{w}_{N_1(\widehat{w}_0)+1}.$$

If we show that $h(\widehat{z}) > m$, then it must be (see also (24) with $z_0 = \widehat{w}_0$)

$$|\lambda_+(\tau^+(\widehat{w}_0))||\lambda_+(\tau)^{N_2(\widehat{w}_0)+1}| < |\lambda_+(\tau^+(\bar{w}_0^+))||\lambda_+(\tau)^{N_2(\bar{w}_0)}|. \tag{27}$$

Consider first the case $N_1(\widehat{w}_0) = N_1(\bar{w}_0)-1$. Then, $\widehat{w}_{N_1(\widehat{w}_0)+1} = S_-(\tau)^{N_1(\widehat{w}_0)+1}\widehat{w}_0 = S_-(\tau)^{N_1(\bar{w}_0)}\widehat{w}_0$, and, using the fact that the matrices $S_-(\cdot)$ and $S_+(\cdot)$ commute, we get

$$\begin{aligned}\widehat{z} &= S_+(\tau_+(\bar{x}_\tau^+))S_+(\tau)^{N_2(\bar{w}_0)}\widehat{w}_{N_1(\widehat{w}_0)+1} \\ &= S_+(\tau_+(\bar{x}_\tau^+))S_+(\tau)^{N_2(\bar{w}_0)}S_-(\tau)^{N_1(\bar{w}_0)}\widehat{w}_0 \\ &= S_-^{-1}(\tau_-(\bar{x}_\tau^-))\left[S_+(\tau_+(\bar{x}_\tau^+))S_+(\tau)^{N_2(\bar{w}_0)}S_-(\tau)^{N_1(\bar{w}_0)}S_-(\tau^-(\bar{x}_\tau^-))\right]\widehat{w}_0,\end{aligned}$$

from which (since the term in square brackets is the identity) $S_-(\tau_-(\bar{x}_\tau^-))\widehat{z} = (\widehat{x}_0^-, m)^T$. This last relation gives $e_2^T\widehat{z} = \frac{m+\tau_-(\bar{x}_\tau^-)(cm+d\widehat{x}_0^-)}{1+2\tau_-(\bar{x}_\tau^-)c+(\tau_-(\bar{x}_\tau^-))^2(c^2+d^2)}$. From this, we get $e_2^T\widehat{z} > m$ if $\widehat{x}_0^- > \frac{c}{d}m + \tau_-(\bar{x}_\tau^-)\frac{m}{d}(c^2+d^2)$ which is true for τ sufficiently small.

If $N_1(\widehat{w}_0) = N_1(\bar{w}_0) - 2$, then $\widehat{w}_{N_1(\widehat{w}_0)+1} = S_-(\tau)^{N_1(\bar{w}_0)}\alpha\bar{w}_0$, with α as in (22). Then

$$\begin{aligned}\widehat{z} =& \alpha S_-(\tau_-(\bar{x}_\tau^-))^{-1}[S_+(\tau_+(\bar{x}_\tau^+))S_+(\tau)^{N_2(\bar{w}_0)}S_-(\tau_-(\bar{x}_\tau^-))S_-(\tau)^{N_1(\bar{w}_0)}]\bar{w}_0 \\ =& \alpha S_-(\tau_-(\bar{x}_\tau^-))^{-1}\bar{w}_0,\end{aligned}$$

if and only if $S_-(\tau_-(\bar{x}_\tau^-))\widehat{z} = \alpha\begin{bmatrix}\bar{x}_\tau^- \\ m\end{bmatrix}$ and this gives $e_2^T\widehat{z} = \alpha\frac{m+\tau_-(\bar{x}_\tau^-)(cm+d\bar{x}_\tau^-)}{1+2\tau_-(\bar{x}_\tau^-)c+(\tau_-(\bar{x}_\tau^-))^2(c^2+d^2)}$. From this, we will surely get $e_2^T\widehat{z} > m$ if $\bar{x}_\tau^- > \frac{c}{d}m + \tau_-(\bar{x}_\tau^-)\frac{m}{d}(c^2+d^2)$ which is true for τ sufficiently small.

Inequality (25) and (27) together imply that (see equation (20)),

$$|\lambda_+(\tau(\widehat{w}))||\lambda_+(\tau)^{N_2(\widehat{w}_{N_1(\widehat{w}_0)+1})}||\lambda_-(\tau)^{N_1(\widehat{w}_0)+1}| < |\lambda(\tau, \bar{x}_\tau^-)| = 1.$$

The proof for $\widetilde{w}$ carries on in a similar way. □

Below, if $w \in \Sigma^-$, we will denote with (x_k^-, m) and with (x_k^+, m), $k \geq 0$, the intersection points of $\gamma_{t,\tau}(w)$ respectively with Σ^- and Σ^+. The notation is chosen so that $(x_{k+1}^\pm, m)$ (if it exists), is the intersection point immediately subsequent to $(x_k^\pm, m)$.

Theorem 16. *For any $w \in \Sigma^-$ and for τ sufficiently small, there exists $K(\tau) > 0$ such that, for $k > K(\tau)$, the points x_{2k+1} are contained in $[\widetilde{x}_1^-, \widehat{x}_1^-]$.*

Proof. Let $w = (x_0^-, m) \in \Sigma^-$. Following the same reasonings as in the proof of Lemma 15 , if $x_0^- > \widehat{x}_1$, then $x_1^- < x_0^-$. Moreover there must be a $K > 0$ such that $x_{2K+1}^- < \widehat{x}_1$. Indeed, if this were not the case, the sequence x_{2k+1}^- would be montone decreasing and bounded below by $\widehat{x}_1^-$ and hence it would converge to a point $x^- \geq \widehat{x}_1^-$. Now, take $w^- = (x^-, m)$ and consider the sequence of intersection points of $\gamma_{t,\tau}(w^-)$ with Σ^-. Because of Lemma 15, it must be $x_1^- < x^-$. A contradiction. The proof for $x_1 > \widetilde{x}_1$ is similar. □

The proof of Claim 1 follows from the fact that the interval $\omega(\tau)$ relative to the cross section $y = m$, satisfies $\omega(\tau) \subset [\widetilde{x}_1^-, \widehat{x}_1^-]$ and $[\widetilde{x}_1^-, \widehat{x}_1^-] = O(\tau)$. □

Corollary 17. *The band-like region obtained applying Euler method to (1) contains the periodic orbit of the method with event search γ_τ. Moreover it converges to γ as τ goes to 0.*

Proof. The proof follows upon noticing that $\bar{x}_\tau^- \in [\widetilde{x}_1^-, \widehat{x}_1^-]$ and that $\gamma_\tau \to \gamma$ as $\tau \to 0$. This implies $\lim_{\tau\to 0} \widetilde{x}_1^- = \lim_{\tau\to 0} \widehat{x}_1^- = \bar{x}^-$. □

Example 18. Although we only analyzed planar problems, the "band" phenomenon which we observed in those cases seems to be a general feature of discretizations of discontinuous systems having a periodic orbit. To witness, below we show results obtained for the well known Chua's circuit in its discontinuous formulation. The system is in $\mathbb{R}^3$, and given by

$$\frac{dx}{dt} = \begin{cases} \begin{bmatrix} -\alpha - \alpha m_1 & \alpha & 0 \\ 1 & -1 & 1 \\ 0 & -\beta & 0 \end{bmatrix} x + \begin{bmatrix} \alpha(m_0 - m_1) \\ 0 \\ 0 \end{bmatrix}, & x_1 < -1\,, \\ \begin{bmatrix} -\alpha - \alpha m_0 & \alpha & 0 \\ 1 & -1 & 1 \\ 0 & -\beta & 0 \end{bmatrix} x\,, & -1 < x_1 < 1\,, \\ \begin{bmatrix} -\alpha - \alpha m_1 & \alpha & 0 \\ 1 & -1 & 1 \\ 0 & -\beta & 0 \end{bmatrix} x + \begin{bmatrix} \alpha(m_1 - m_0) \\ 0 \\ 0 \end{bmatrix}, & x_1 > 1\,, \end{cases} \tag{28}$$

where we take $\alpha = 15.6$, $\beta = 50$, $m_0 = -8/7$, $m_1 = -5/7$, for which it is known that the discontinuous system has two crossing periodic orbits (see [1], Sec 9.4). Results obtained with Euler method (with constant stepsize) are in Figure 7.

4. **Conclusions.** In this work, we considered a model planar piecewise linear system with an attracting periodic orbit, and studied what happens to a Euler discretization with stepsize τ of this piecewise linear system. In contrast to standard results for smooth systems, we showed that the discrete system trajectories remain inside a band, whose width is proportional to the discretization stepsize τ. (In the smooth case, for τ sufficiently small, the discrete system has an invariant curve).

We also considered a smooth regularization of the piecewise linear system. After rewriting it in polar coordinates, we considered its Euler discretization, and gave evidence that the discrete solution undergoes a period doubling cascade with respect to the regularization parameter ϵ, for fixed τ.

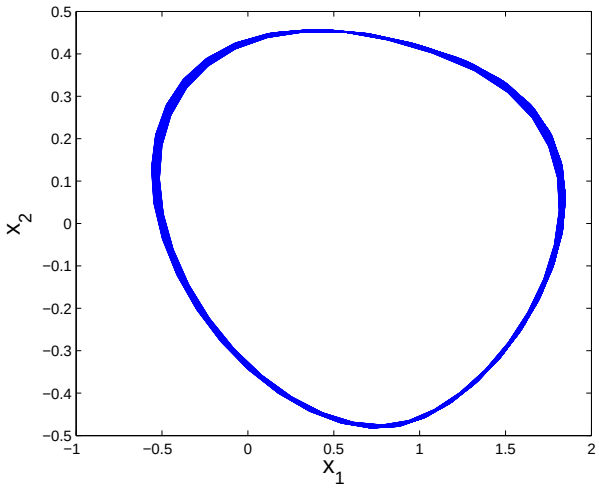

FIGURE 7. Example 18: Euler approximation for $\tau = 0.03$.

Finally, we proved that an event-driven Euler discretization of the model problem has a discrete periodic solution near the one of the original problem, for sufficiently small τ.

We have only considered the Euler discretization, the prototypical one-step scheme, and a model piecewise linear system. Although it is possible that different discretizations, and systems, give somewhat different results, we expect that our results are indicative of the following general paradigm.

(i) When considering discretization of discontinuous systems with an attractive periodic orbit, the standard results from the smooth case do not carry over, in particular the discretazion of the discontinuous system does not generally have an invariant curve, which gets replaced by an invariant band.

(ii) However, when enforcing an event search, then the resulting event-driven-method approximates periodic solutions to the order of the method.

REFERENCES

[1] K. T. Alligood, T. D. Sauer and J. A. Yorke, *Chaos*, Springer-Verlag, New York, 1997.

[2] W.-J. Beyn, On invariant closed curves for one-step methods, *Numerische Mathematik*, **51** (1987), 103–122.

[3] L. Dieci, C. Elia and D. Pi, Limit cycles for regularized discontinuous dynamical systems with a hyperplane of discontinuity, *DCDS-B,* **22** (2017), 3091–3112.

[4] L. Dieci and C. Elia, Periodic orbits for planar piecewise smooth dynamical systems with a line of discontinuity, *Journal of Dynamics and Differential Equations,* **26** (2104), 1049–1078.

[5] L. Dieci and L. Lopez, A survey of Numerical Methods for IVPs of ODEs with Discontinuous right-hand side, *Journal of Computational and Applied Mathematics,* **236** (2012), 3967–3991.

[6] T. Eirola, Invariant curves of one-step methods, *BIT,* **28** (1988), 113–122.

[7] J. Sotomayor and A. L. Machado, Structurally stable discontinuous vector fields on the plane, *Qual.Theory of Dynamical Systems,* **3** (2002), 227–250.

[8] J. Sotomayor and M. A. Teixeira, Regularization of discontinuous vector fields, *International Conference on Differential Equations, Lisboa*, (1998), 207–223.

[9] A. Stuart and A. R. Humphries, *Dynamical Systems and Numerical Analysis*, Cambridge University Press, 1996.

Received February 2017; revised November 2017.

E-mail address: dieci@math.gatech.edu
E-mail address: cinzia.elia@uniba.it